

A novel multirobot map fusion strategy for occupancy grid maps

Sebahattin TOPAL^{1,*}, İsmet ERKMEN², Aydan Müşerref ERKMEN²

¹Department of Electronic and Communication Engineering, Süleyman Demirel University,
32260 Isparta, Turkey

²Department of Electrical and Electronics Engineering, Middle East Technical University,
06800 Ankara, Turkey

Received: 09.06.2011 • Accepted: 22.09.2011 • Published Online: 27.12.2012 • Printed: 28.01.2013

Abstract: In this paper, we consider the problem of merging partial occupancy grid environment maps, which are extracted independently by individual robot units during search and rescue (SAR) operations in complex disaster environments. Moreover, these maps are combined using intensity-based and area-based features without knowing the initial position and orientation of the robots. Our proposed approach handles the limitation of existing studies in the literature; for example, the limited overlapped area between partial maps of robots is enough for good merging performance and unstructured and complex partial environment maps can be merged efficiently. These abilities allow multirobot teams to efficiently generate the occupancy grid map of catastrophe areas and localize buried victims in the debris as soon as possible. The simulation results support the potential of the proposed multirobot map fusion methodology for SAR operations in unstructured, complex, and completely unknown disaster environments.

Key words: Map fusion, multirobot systems, occupancy grid mapping, search and rescue

1. Introduction

Search and rescue (SAR) operations can be hostile to human beings working within catastrophe areas due to unstable structures and/or the leakage of dangerous gas or nuclear fumes, which are the general characteristics of urban area disasters. Moreover, human fatigue and even exhaustion are very common adversaries to time-critical SAR operations. Hence, robot usage, instead of human beings and trained dogs, becomes a must in these dangerous missions, thus reducing the probability of human rescuers being injured and increasing the efficiency in time-critical endeavors. Consequently, the exploration of unknown and complex disaster environments using robot teams has gathered wide attention during the past decade, especially in the field of SAR robotics. Robot units in the team face various challenging problems due to hard and dangerous environmental conditions, like the self-localization of each robot and disaster area map generation. These challenges have led to the emergence of the new research topic of simultaneous localization and mapping (SLAM), where the most recent research is focused. The accurate estimation of robot location and the map building of an explored region have found many different applications, among which SAR occupies the greater challenge, being real-time in a highly uncertain region [1,2]. Especially for SAR operations in wide, unstructured, and hardly known catastrophe environments, mapping, which is the process of incrementally extracting a map of the surrounding, is a very crucial job to be undertaken during the autonomous navigation of robots. SAR multirobot systems are often suggested for mapping tasks due to many advantages, such as energy and time efficiency over single robot systems [3–6].

*Correspondence: sebahattintopal@sdu.edu.tr

The efficiency of the system comes from the coordination and cooperation between robot units, leading to the integration of partial maps that are generated by robot team members operating in different parts of the same mission area, which leads to highly disparate maps when catastrophe areas are large. Each robot enters the work space from totally separate regions and independently explores and extracts the maps of different parts of the environment. When such robots exchange their partial maps of their exploration surroundings, it becomes extremely difficult to merge them, since the initial position and orientation of each robot is not known by other robots, i.e. each robot's reference frames for mapping are different. Hence, map merging problems in these situations are attempted after a preprocessing through translation and rotation that tries to align the robots' local mapping frames. The preprocessing steps generally include the computation of the translational and rotational difference between the robots' maps, followed by the map of one robot being rotated and translated with respect to another robot's map taken as the first priority. Map merging for a large environment based on multirobot systems still remains a challenge and if such a merging could acquire high accuracy, which is still the focus of many present-day studies, disaster area coverage would be achieved in a decentralized manner, generating the inventory of the disaster and leading to a faster localization of possible survivors.

Many researchers have worked on merging maps obtained by individual robots that start exploration from different parts of the same environment and extract the map of the surroundings independently with respect to their own reference frames. Some simplifications are brought to the problem by basing the map merging on features such as doors, junctions, and corners [7,8]. Although these studies have demonstrated the success of feature-based map merging methods for multirobot systems, these approaches remain unfeasible for unstructured and complex work environments, because feature extraction is very hard to carry out in such unstructured areas where prior information does not exist. Hence, some researchers have focused on occupancy grid-based mapping approaches for modeling the environment and merging the partial robots' maps [9,10]. The occupancy of each grid cell is a numerical value representing the posterior probability of the cell being occupied, estimated independently from the other cells. This provides a simple spatial representation of the environment.

Thus far, several map merging methods have been proposed for occupancy grid maps generated by autonomous robots. Carpin et al. [9] developed an iterative method to combine partial environment maps, in which the map of the second robot is translated and rotated in the space of possible rigid transformations on the map of the first robot, with the aim of maximizing the overlapped region between the robot maps using a similarity metric. This approach guaranteed the finding of the optimal solution when the number of map merging iterations tends to infinity, which is not feasible for real-time and complex applications like SAR operations where time is critical and extremely bounded. In order to improve the efficiency of the proposed algorithm in the sense of time, Carpin [10] presented a new noniterative and fast method using the spectral information of maps. The Hough transform is performed to detect the orientation of each occupancy grid map and the translation information is obtained from 2 signals that are the projections along the x and y directions of the 2 maps. Although this spectral information-based technique is fast and accurate compared to the previous iteration-based method, it also still has some limitations. In this method, it is essential that the 2 partial occupancy grid maps being merged exhibit a certain degree of an overlapping region in order for successful map merging. Moreover, the mapped environment has to be well structured, which means that the mapping area consists of only walls and corridors, not only obstacles. Hence, these limitations, especially the second one, make the proposed occupancy grid map merging methodology unfeasible for unstructured and complex SAR areas like collapsed buildings due to earthquakes, where walls and corridors are nonexistent within the rubble.

To handle these limitations, we present a novel occupancy grid map merging method based on intensity-

based and area-based key-point selection and matching. The main contribution of this work is that our proposed algorithm is capable of merging partial maps that have a very limited degree of overlapping regions; this ability increases the efficiency of the system. The presented map merging method works well in unstructured, complex, and initially completely unknown environments like collapsed buildings due to earthquakes, and it makes the system suitable for SAR operations.

The remainder of the text is organized as follows: Section 2 defines the occupancy grid-based multi-robot map merging problem characteristics; our proposed map fusion approach is presented in Section 3; the experimental results are given in Section 4; and, finally, Section 5 concludes the paper.

2. Problem characteristics

The most important distinguishing features of disaster environments are their internal structure, which is the rubble structure that renders them highly uncertain and unstructured. Generally, there is no initial information about the location of the obstacles, victims, and overall structural inventory of the area being searched. A SAR mission primarily includes the coverage and mapping of the mission area using multiple autonomous robots of different capabilities. Those robots enter the vast disaster region from different parts, bearing different initial orientations and positions, and will start their individual exploration mission generating their own occupancy grid environment maps based on their local reference frame. Hence, the mapping frames of each robot are different compared to other members of the robot team and a rotational and translational difference occurs between the generated occupancy grid environment maps.

To increase the efficiency of the decentralized exploration task in the sense of time and energy, robots exchange their partial maps extracted from different parts of the work area. Those maps are then merged toward a globally consistent map of the disaster area by the ground station or each robot unit. If SAR robots know their relative initial positions and orientations, the alignment of the individual local maps will become trivial; however, this assumption is not valid in real-world applications such as SAR operations in disaster areas, and so this assumption is not used in our problem. The problem of map merging using partial maps can be looked upon as the problem of fusing local map pairs without any information about the robots' mapping frames. Each robot has a different reference frame that usually sets their starting position and orientation. In our study, the relative position and rotation information between the robots are not available, and for successful map merging, partial robot maps have to possess only limited overlapping regions, detected only after the individual exploration of the same region by robots.

Another characteristic of multirobot SAR operations is related to the uncertainties about the robots' distance measurements. During the exploration operation, some sensors can crash or their noise bounds can vary according to time. Another source of uncertainty is about signals; communication and distance measurement signals are generally scattered within the rubble and can easily be obstructed in the disaster area. Finally, the ground station has to merge partial occupancy grid maps under the different sensor models and noise bounds of different robots.

3. Methodology

In our multirobot exploration task, we use an occupancy grid map model to represent the internal structure of the disaster area [11]. The environment map is divided into grids and the occupancy of each grid cell is estimated independently. It allows robots to extract the environment map without using any features like corners, walls, or predefined landmarks. The occupancy of a grid is a numerical value representing the posterior probability of the grid cell being occupied. Every grid has 3 states: occupied, free, and unknown. This provides a simple

spatial representation of the environment. Different cell states are represented by different colors. Black cells are related to obstacles and rubble, gray ones show the unknown part of the environment that has not been visited by the robots yet, and the free space, where robots can navigate safely, is represented by white cells. Our proposed multirobot occupancy grid map merging methodology proceeds as in Figure 1. It is based on extracting invariant substructures called key points in the occupancy grid map of disaster areas. Key points, which are invariant to rotation and translation even when generated maps contain a significant amount of noise, have to be located in each robot map. These points, which possess valuable assets for merging maps due to their invariance, are used as a virtual landmark to find the rigid transformation between individual robot maps. Two distinct key-point localization and matching approaches are used, namely intensity-based and area-based. Intensity-based key-point localization gives good performance, especially for robots capable of the same distance measurements. However, robots can have different sensing abilities; for example, some distance measurement sensors can crash during the task execution, or the noise margin of the sensors may be different from that of other robots. Hence, maps of the same environments can be different and intensity-based feature extraction can be limited in these cases, and so area-based key-point localization methodology is proposed to overcome these limitations.

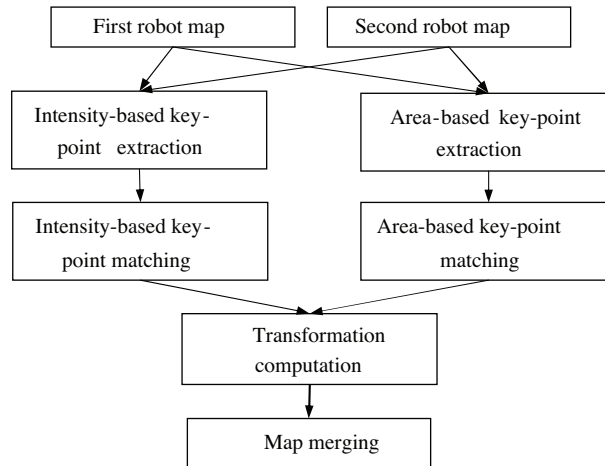


Figure 1. Flow chart of the proposed occupancy grid map merging algorithm.

The selected key points are subsequently matched to label the same explored region between the maps of each robot. A correspondence is thus found between the maps during the matching process, leading to the detection of the following sort: “this point in the first map is related to that point in the second environment map”. Using these correspondence points between the maps, the rotational and translational differences between the maps are calculated and the maps are then merged using the estimated transformation. The details of the above steps of our map merging process are explained in detail in the following subsections, demonstrated within the flow of a simple example.

3.1. Intensity-based key-point localization and matching

In the occupancy grid map merging problem, distinctive and stable key points that are invariant to rotation, translation and noise have to be localized to find the correspondence points between the partial local environment maps of the robots. In the literature, a scale-invariant feature transform algorithm, which is widely applicable in pattern recognition and computer vision, has been proven to be a robust detector of invariant interest points, especially for gray-scale images [11–13]. Hence, it can be used as a powerful key-point extraction tool in the map

merging task. In our approach, the scale-invariant feature transform is used to localize the key points for each occupancy grid map to find the correspondence points between partial robot environment maps. The key-point localization algorithm consists of some important subparts: detection, localization, orientation assignment, and descriptions of the extracted key points. All of these stages are explained in the following subsections in detail.

3.1.1. Scale-space extreme detection

This first step is the identification of potential distinctive interest points that are invariant to orientation, translation, and scaling using a difference of Gaussian (DoG) function, and these points also have to be stable towards noise. The local extremes of the DoG filters at different scales are used to identify potential interest points. These points are located at scale-space maxima/minima across different scales of a DoG function. The DoG of a robot map $M(x, y)$ is calculated as in Eq. (1):

$$\begin{aligned} D(x, y, \sigma) &= (G(x, y, k\sigma) - G(x, y, \sigma)) * M(x, y) \\ &= L(x, y, k\sigma) - L(x, y, \sigma), \end{aligned} \quad (1)$$

where $M(x, y)$ is the occupancy grid environment map generated by the robot units and $L(x, y, \sigma)$ is the scale space representation of it, and x and y are the pixel coordinates in the x and y directions of the map, respectively. The factor represented as k is used for changing the scale, $G(x, y, \sigma)$ is the Gaussian filter that is used for smoothing the map image, and σ is the width of the filter. In order to detect the local maxima and minima of the DoG filter $D(x, y, \sigma)$, each sample point is compared to its 8 neighbors in the current image and 9 neighbors in the scale above and below. It is only selected as a candidate key point if it is larger than all of these neighbors or smaller than all of them. This procedure provides the localization of maxima points in the images that are passed through the DoG filter. Some example key points of an occupancy grid environment map are shown by red stars in Figure 2.

3.1.2. Key-point localization, orientation assignment, and description

The basic idea in this subsection is the rejection of key points whose pixels are lower than the predetermined threshold value (0.02) due to their sensitivity to noise. After the extraction of candidate interest-point locations, unreliable key points whose intensities are very low are eliminated. According to this threshold applied to the environment map presented in Figure 2, a “strong” set of key points remaining after the elimination procedure is shown in Figure 3. Key-point detection is very sensitive to noise and so the performance of the map merging algorithm would be affected if noisy maps were considered without this threshold.

The next step is to make a detailed fit with nearby data for location and scale using comparison intensity changes between the key point and its neighborhood pixels. The properties of each key point are computed relative to the key-point orientation, so this provides the rotation invariance property. Orientation and magnitude assignments are done for each key point and its neighbors using the following pixel differences in Eqs. (2) through (5).

$$m(x, y) = \sqrt{m_x(x, y)^2 + m_y(x, y)^2} \quad (2)$$

$$\theta(x, y) = \tan^{-1}\left(\frac{m_x(x, y)}{m_y(x, y)}\right) \quad (3)$$

$$m_x(x, y) = L(x + 1, y) - L(x - 1, y) \quad (4)$$

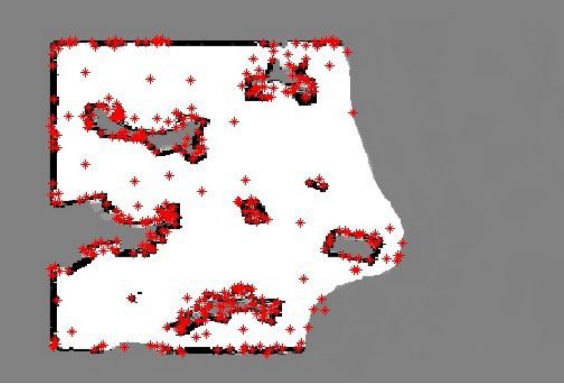


Figure 2. Occupancy grid environment map of the mission space and estimated key points.

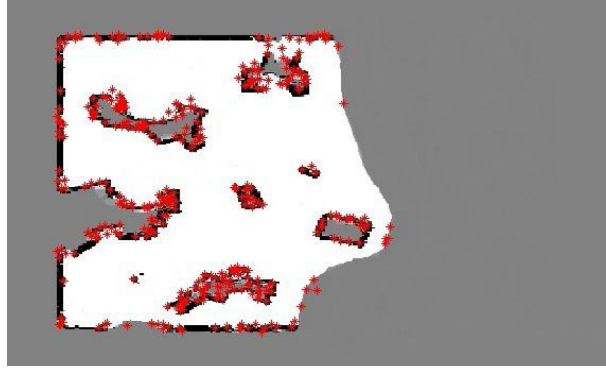


Figure 3. The eliminated key points of the occupancy grid map.

$$m_y(x, y) = L(x, y + 1) - L(x, y - 1) \quad (5)$$

Here, the Gaussian smoothed image is denoted as $L(x, y)$ and the pixel gradient magnitude and orientation are represented by $m(x, y)$ and $\theta(x, y)$, respectively. After the calculation of the gradient orientation and magnitude for each key point and its neighbor pixels, as seen for one case in Figure 4, the orientation of the key point is selected in the direction of the dominant orientation in the neighbor pixel of the key point. The previous stages have assigned orientation for each interest-point location in robot maps $M(x, y)$. The next step is the computation of the key-point descriptor. It is calculated by the gradient magnitude and orientation of the neighbor pixel intensity change gradient vector in a local region around the interest point. A 128-element key-point descriptor is used, using the surrounding gradients of the key point.

3.1.3. Key-point matching

After the calculation of the invariant feature descriptor vector for each key point in the environment map of one robot, they are stored in a database in order to be matched with the occupancy grid environment map of another robot using the nearest neighbor, which is defined as the key point with the minimum Euclidean distance. Since some descriptors are more discriminative than others, a constant threshold cannot eliminate incorrect matching. Adaptive threshold calculation handles the ambiguity problem by comparing the nearest neighbor with the second neighbor, as in Eq. (6). The selection of the threshold on the correspondence matching process is obtained using Figure 5, which shows us the sensitivity of correspondence point matching with the defined threshold in the occupancy grid environment robot maps.

$$\frac{\text{Best match}}{\text{Second best match}} < 0.65 \quad (6)$$

A total of 2000 key points, obtained from different occupancy grid maps of the environment, are used to acquire Figure 5, which shows the probability density functions for correct and incorrect matches using the closest and second nearest neighbor ratio. For our occupancy grid environment map merging operation, we eliminate all correspondence points where the distance ratio is greater than 0.65. We observe from Figure 5 that when the threshold exceeds a value of 0.65, the number of incorrect matches between the maps increases dramatically and the number of correct matches decreases, and so 0.65 is an optimum threshold value for the key-point matching process.

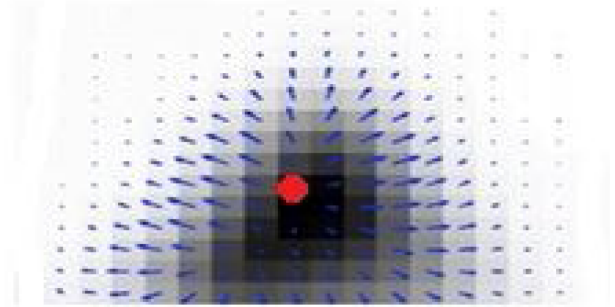


Figure 4. Gradient values in the neighborhood pixels of the key point.

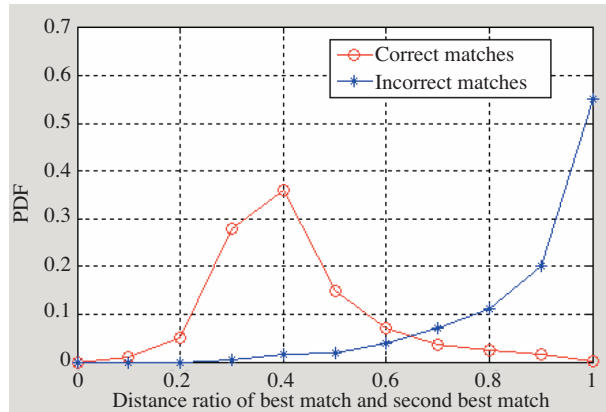


Figure 5. Probability density functions of correct and incorrect matches using the ratio of closest and second closest neighbor for occupancy grid maps.



Figure 6. Partial environment occupancy grid map of the robots: a) first robot and b) second robot.

Figure 7 shows some matched key points between the maps of robots after the implementation of the above procedure. Correct key-point matches are represented by blue lines and incorrect ones are represented by red lines. When the number of incorrect matches increases due to sensor failure or noise bound, map merging cannot be done. Hence, to increase the performance of the map merging task, an area-based key-point selection and matching methodology is presented in Subsection 3.2 and incorrect key-point matching elimination and transformation estimation between the robots' maps is presented in Subsection 3.3.

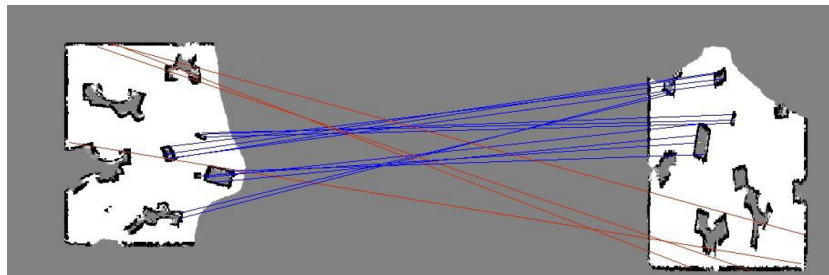


Figure 7. Key-point matching between the partial robot maps.

3.2. Area-based feature extraction

The performance of the intensity-based key-point localization and matching method described above is sufficient when the number of key points is enough for a merging occupancy grid map of robots with almost the same

measurement capability. However, some sensors can crash or the noise rate of the sensors can vary during the task execution, and so some parts of the maps obtained by one robot can be different from another, such as in Figures 8a and 8b. There are some intensity differences between the maps of the same obstacle, seen in the difference map of Figure 8c. Intensity-based methodology cannot localize enough correct and stable key points because of different sensing ranges and error bounds. Hence, we need more feature points and obstacle-related areas are used as connected components, which are the group of black pixels in the binary image. We use a hybrid key-point extraction methodology that consists of area-based and intensity-based features. Area-based key-point extraction and matching is described below.



Figure 8. Obstacle map, extracted by robots with different sensing capabilities: a) first robot, b) second robot, and c) difference.

Our work environment is unstructured and so there are many obstacles (connected components) that can give extra information about the translational and rotational differences between robot maps. Connected component analysis is used to extract the orientation and location of the obstacles that are then used as extra features, using the following procedure:

- i. The occupancy grid environment map is the threshold to yield a binary map that is a simplified version of the occupancy grid map, and the connected components can be found more precisely than the original ones.
- ii. A 2-pass algorithm [14] is used to detect closed boundary regions, which are about the obstacle-related area. The first pass of the algorithm finds equivalences and assigns temporary labels to each pixel and the second pass is required for finding the remaining equivalences and final labeling.
- iii. After the detection of the connected components, which are related to the obstacles, we extract some features such as the center of mass, area, and orientation of the connected component. The center of mass is calculated using the following equation:

$$\bar{x} = \frac{\iint xb(x,y)dxdy}{\iint b(x,y)dxdy}, \quad \bar{y} = \frac{\iint yb(x,y)dxdy}{\iint b(x,y)dxdy}, \quad (7)$$

where $b(x,y) = 0$ for the background and $b(x,y) = 1$ for the connected component-related area. The area and orientation of each connected component is calculated using Eqs. (8) and (9), respectively.

$$A = \iint b(x,y)dxdy \quad (8)$$

$$\tan 2\theta = \frac{b}{a-c}, \quad a = \iint (x')^2 b(x',y') dx' dy' \quad (9)$$

$$b = 2 \iint (x'y') b(x',y') dx' dy' \quad c = \iint (y')^2 b(x',y') dx' dy' \quad (10)$$

Here, x' and y' are about the obstacles' center of mass in the x and y directions, respectively.

The centers of mass of similar components are used as key-point locations. Since the area of the connected component is rotation- and transitional-invariant, we can obtain similar connected components using the nearest neighbor of the area of connected components based on Euclidean distance. Hence, each robot has intensity- and area-based key points and their correspondences into other maps. The translational and rotational difference, or transformation, between the robot maps is estimated using the following procedure in Subsection 3.3.

3.3. Transformation computation

Transformation between robot maps in order to align them can be estimated precisely when all of the correspondence points are correct. However, there exist some incorrectly matched key points between the occupancy grid maps. Correct matches are called inliers and incorrect ones called outliers. Hence, to combine partial robot maps, we have to eliminate the outliers from all of the correspondence point space. The random sample consensus [15] algorithm, which is a probabilistic parameter estimation method, is used to discard incorrect matches. In this methodology, 2 correspondence pairs, $[x_1, y_1] [x'_1, y'_1]$ and $[x_2, y_2] [x'_2, y'_2]$, are selected randomly from the correspondence point space, and if these points are obtained using the intensity-based key-point localization algorithm described in Subsection 3.1, the transformation parameters are calculated using Eq. (11) for orientation and Eq. (12) for translation estimation.

$$\theta = \text{atan} \frac{(\beta\gamma - \alpha\sigma)}{(\alpha\beta + \sigma\gamma)} \quad (11)$$

$$t_x = x'_1 - \cos(\theta) x_1 + \sin(\theta) y_1, t_y = y'_1 - \sin(\theta) x_1 - \cos(\theta) y_1 \quad (12)$$

Here, $\alpha = (x'_1 - x'_2)$, $\beta = (x_1 - x_2)$, $\gamma = (y'_1 - y'_2)$ and $\sigma = (y_1 - y_2)$. If randomly selected correspondence points are obtained using the area-based key-point localization method described in Subsection 3.2, orientation is obtained by taking the difference of the matched connected components' orientations and the translation is estimated by subtracting the center of their mass in the x and y axes. Next, all of the key points in the second map are transformed into the first map using calculated transformation and error in the sense of Euclidian distance is calculated using the distance between the key points of the first map and transformed key points of the second map. The above procedure continues until the number of predetermined iterations is terminated and the transformation parameters are selected with minimum error at the end of the iteration procedure.

3.4. Map merging

Once the transformation matrix T , as in Eq. (13) between the reference frames of the robots, is calculated as in Subsection 3.3, the second robot's environment map is transformed using Eq. (14), such that it aligns with the first robot's map. The transformed occupancy grid map of the second robot, M'_2 , can then easily be fused with the first robot's map using Eq. (15). If any pixel (x,y) is not located in the overlapped area, its intensity value remains the same; otherwise, the weighted sum of the pixel intensities is used to obtain the overlapped area.

$$T = \begin{bmatrix} \text{Cos}(\theta) & -\text{Sin}(\theta) & \Delta_x \\ \text{Sin}(\theta) & \text{Cos}(\theta) & \Delta_y \\ 0 & 0 & 1 \end{bmatrix} \quad (13)$$

$$M'_2 = \begin{bmatrix} 1 & 0 & 0 \\ 0 & 1 & 0 \end{bmatrix} \cdot T(\Delta_x, \Delta_y, \theta) \cdot M_2 \quad (14)$$

$$M(x, y) = \begin{cases} M_1(x, y) & (x, y) \in M_1 \\ \alpha M_1(x, y) + \beta M'_2(x, y) & (x, y) \in M_1 \cap M'_2 \\ M'_2(x, y) & (x, y) \in M'_2 \end{cases} \quad (15)$$

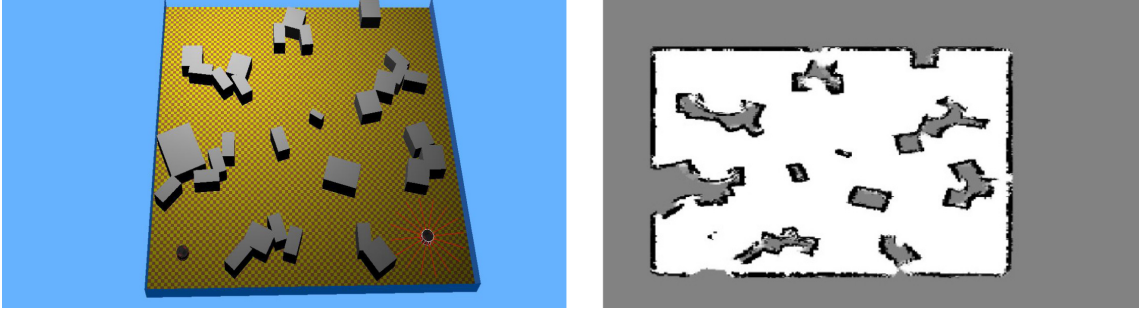


Figure 9. Disaster area (a) and its occupancy grid map (b), as obtained by our proposed map merging methodology.

Here $0 < \alpha\beta < 1$ and $\alpha + \beta = 1$; these are called the measure of reliability and their values are given to the system by the user according to the noise margin of the related robot's distance measurements. After the above procedure, the generated occupancy grid robot maps are merged using the proposed method and the resultant global map of the work environment (Figure 9a) is obtained, as in Figure 9b. The map merging performance results are discussed in detail in the following section.

4. Simulation results

To evaluate our approach, we performed a victim search scenario, as seen in Figure 10. Consider a SAR scenario in a complex and unknown disaster environment like a semicollapsed wide building after an earthquake. The simulation environment is constructed with a 150×150 square area using the Webots [16] commercial mobile robot software developed by Cyberbotics. There are many obstacles, represented by the color gray, scattered randomly into the environment. Their sizes, orientations, and positions are completely different due to the model catastrophe area. Two Magellan robots, equipped with 16 infrared distance sensors with limited sensing range, are deployed for the survivor SAR operation. They have autonomous navigation and map extraction abilities with different sensor noise bounds.

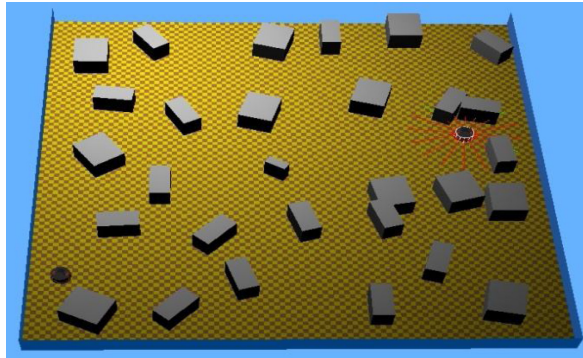


Figure 10. Complex and unstructured disaster area.

Their main goal is to generate the internal structure of the work space and localize buried victims as soon as possible using SLAM and occupancy grid map merging abilities. Hence, each robot starts to explore the environment, starting from its initial position. They construct the map of the work area with respect to their own reference frames, which are different for each robot. Hence, rotational and translational differences occur between the occupancy grid maps of the robot team members, such as in Figure 11. To obtain a joint and global environment map representation, the second robot's map has to be rotated 90° in a clockwise direction and translated with proper values in the x and y directions.

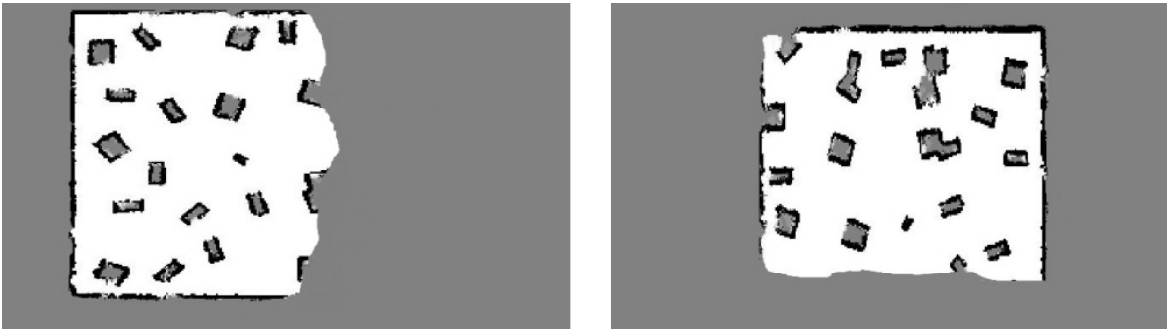


Figure 11. Partial environment map of each robot: a) first robot and b) second robot.

During the SAR operation, the robots notice each other via communication ability. They exchange their local maps to obtain a global map (Figure 12) and the knowledge of each robot about other parts of the environment increases. Hence, the efficiency of the overall system is improved in the sense of time and energy. In order to calculate rigid transformation between the partial occupancy grid maps, the correspondence points between each robot's partial maps are selected and the partial occupancy grid maps of the robots are merged using our proposed methodology described above.

In this section, several experiments are performed to evaluate the effectiveness of the proposed partial occupancy grid environment map merging methodology using disaster areas. Figure 13 shows us the sensitivity of our proposed method to the overlapping area percentage between the occupancy grid maps to be merged. The sensitivity is evaluated in terms of the estimated transformation error, i.e. map merging error per overlapping percentage. We can see from Figure 13 that if we try to merge maps when the percentage of overlapped area between the maps is 0%, the merging error is approximately 100%. This is because the robots did not navigate into the same area; thus, there is no overlapped area between the maps and no correct correspondence points can be generated as virtual landmarks. If we increase the percentage of overlapped area between the robot maps, the merging error decreases dramatically and 30% overlapped area can be enough for the occupancy grid map merging operation in the desired error range. When the robots explore exactly the same area, they extract similar maps, and so the overlapped area percentage is approximately 100% and the map merging error converges to approximately 0%.

Another experiment is performed to test the map merging ability of our proposed method with 2 robots that have different noise bounds. In the simulation experiments, each robot has a different noise model. For example, the first robot has a 10% uniform noise margin in its distance measurements, while the second robot's noise margin is 15%; hence, there occurs a 5% noise bound difference between the robot distance measurements. This noise difference causes different environment map models for some regions.

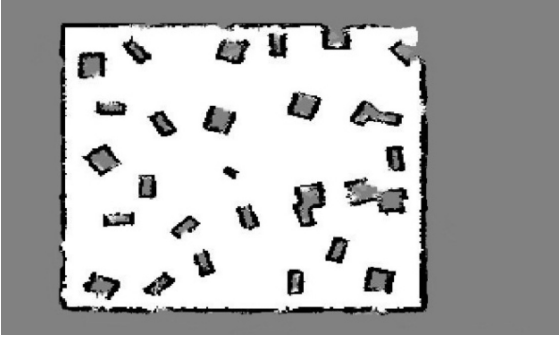


Figure 12. Occupancy grid environment map of the SAR space.

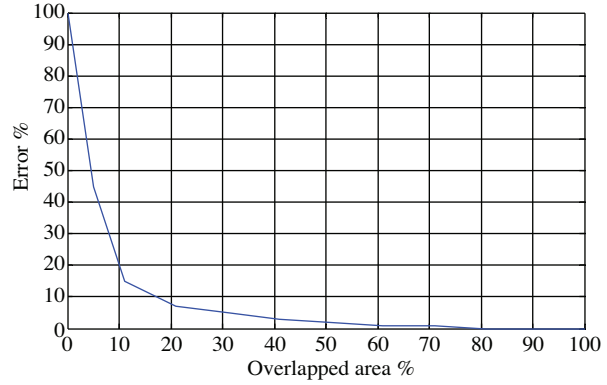


Figure 13. Map merging error according to the overlapped area between the maps.

We observe from Figure 14 that if there is no difference between the robots' noise bounds, the occupancy grid map merging error is very small, and when the noise bound difference between the robots' distance sensor measurements increases, the map merging error remains within tolerable limits, up to 40%. When the noise bound difference increases to 100%, map merging cannot be done due to the huge amount of transformation estimation, and so an intolerable map merging error occurs.

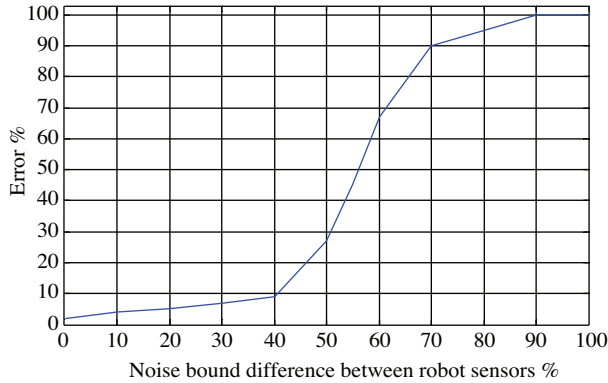


Figure 14. Map merging error according to the noise bound difference between the robots.

5. Conclusion

Map merging is a challenging task, especially for real-time multirobot SAR operations in disaster environments. Combining the partial maps of robots into a global one allows the robot team to avoid repeated exploration of some regions by different robots. In this paper, we introduced a novel map merging methodology for occupancy grid maps to obtain a global and consistent environment map for multirobot exploration operations in SAR environments. The proposed approach handles the limitations of existing studies in the literature, such as disaster areas like semicollapsed buildings due to earthquakes that are completely unknown and unstructured. Hence, we propose a map fusion methodology that can be used not only for mapping in structured environments, but can also be used efficiently in unstructured and complex environments. The presented algorithm is also capable of successfully merging the partial occupancy grid map of robots that have a limited degree of overlapping regions between their maps.

References

- [1] W. Burgard, M. Moors, C. Stachniss, F.E. Schneider, “Coordinated multi-robot exploration”, *IEEE Transactions on Robotics*, Vol. 21, pp. 376–386, 2005.
- [2] D. Fox, J. Ko, K. Konolige, B. Limketkai, D. Schulz, B. Stewart, “Distributed multi-robot exploration and mapping”, *Proceedings of the IEEE*, Vol. 94, pp. 1325–1339, 2006.
- [3] C. Stachniss, “Exploration and mapping with mobile robots”, PhD Dissertation, Computer Engineering Department, Freiburg University, 2006.
- [4] R. Zlot, A. Stentz, M. Dias, S. Thayer, “Multi-robot exploration controlled by a market economy”, *Proceedings of the IEEE International Conference on Robotics and Automation*, Vol. 3, pp. 3016–3023, 2002.
- [5] L. Bayındır, E. Şahin, “A review of studies in swarm robotics”, *Turkish Journal of Electrical Engineering & Computer Sciences*, Vol. 15, pp. 115–147, 2007.
- [6] S.N. Givigi Jr, H.M. Schwartz, “Swarm robot systems based on the evolution of personality traits”, *Turkish Journal of Electrical Engineering & Computer Sciences*, Vol. 15, pp. 257–282, 2007.
- [7] K. Konolige, D. Fox, B. Limketkai, J. Ko, B. Stewart, “Map merging for distributed robot navigation”, *Proceedings of the IEEE International Conference on Intelligent Robots and Systems*, pp. 212–217, 2003.
- [8] N. Adluru, L.J. Latecki, M. Sobel, R. Lakaemper, “Merging maps of multiple robots”, *Proceedings of the 19th International Conference on Pattern Recognition*, pp. 1–4, 2008.
- [9] S. Carpin, A. Birk, V. Jucikas, “On map merging”, *Robotics and Autonomous Systems*, Vol. 53, pp. 1–14, 2005.
- [10] S. Carpin, “Fast and accurate map merging for multi-robot systems”, *Autonomous Robots*, Vol. 25, pp. 305–316, 2008.
- [11] A. Elfes, “Using occupancy grids for mobile robot perception and navigation”, *IEEE Computer*, Vol. 22, pp. 46–57, 1989.
- [12] D.G. Lowe, “Distinctive image features from scale-invariant key points”, *International Journal of Computer Vision*, Vol. 60, pp. 91–110, 2004.
- [13] C. Belcher, Y. Du, “Region-based SIFT approach to iris recognition”, *Optics and Lasers in Engineering*, Vol. 47, pp. 139–147, 2009.
- [14] L. Shapiro, G. Stockman, *Computer Vision*, New Jersey, Prentice Hall, pp. 69–73, 2002.
- [15] M.A. Fischler, R.C. Bolles, “Random sample consensus: a paradigm for model fitting with applications to image analysis and automated cartography”, *Communications of the ACM*, Vol. 24, pp. 381–395, 1981.
- [16] Webots, Commercial mobile robot simulation software, <http://www.cyberbotics.com>.